J Solid State Electrochem (2016) 20:215–223
DOI 10.1007/s10008-015-3019-0

ORIGINAL PAPER

One-step solid-state synthesis of $Li_4Ti_5O_{12}$/C with low in situ carbon content and high rate cycling performance

Yonglong Zhang[1] · **Ziji Lin**[3,4] · **Xuebu Hu**[1,2] · **Ping Cao**[1,2] · **Yaoqiong Wang**[1]

Received: 5 May 2014 / Revised: 26 April 2015 / Accepted: 15 August 2015 / Published online: 29 August 2015

Abstract Spinel $Li_4Ti_5O_{12}$/C composites were obtained from $C_3H_5O_3Li$ and TiO_2 via one-step solid-state reaction without adding extra carbon sources. This facile synthesis method can reduce production steps, contribute to uniform mixing of raw materials, and get homogenous particles. As-prepared $Li_4Ti_5O_{12}$/C composites with low in situ carbon content of only 1.81 wt% show significant improvement in discharge capacity and high rate cycling performance comparable to $Li_4Ti_5O_{12}$/C in previous studies, showing that low in situ carbon content in the as-prepared $Li_4Ti_5O_{12}$/C composites perfectly balances discharge capacity and high rate cycling performance. At 1 C and 10 C, the initial discharge capacity is 168.0 and 140.0 mAh g^{-1} with capacity retention of 94.4 and 90.2 % after 200 cycles, respectively. Even at 20 C, the discharge capacity is 133.3 mAh g^{-1} at 1st cycle and 109.8 mAh g^{-1} at 50th cycle. It demonstrated promising potential as an anode material in lithium-ion batteries with excellent discharge capacity and high rate cycling performance.

✉ Xuebu Hu
xuebu8006@126.com

[1] College of Chemistry and Chemical Engineering, Chongqing University of Technology, Chongqing 400054, People's Republic of China

[2] Chongqing Enterprise Engineering Technology Research Center for Phosgene Derivatives, Changshou, Chongqing 401252, People's Republic of China

[3] Sichuan Provincial Centre for Quality Supervision & Inspection of Alcohol Packaging Products, Luzhou, Sichuan 646000, People's Republic of China

[4] Luzhou Products Quality Supervision & Inspection Institute, Luzhou, Sichuan 646000, People's Republic of China

Keywords $Li_4Ti_5O_{12}$/C · One-step solid-state synthesis · High rate cycling performance · Low in situ carbon content · Lithium lactate

Introduction

Nowadays, exploration of a new anode material with high safety and excellent cyclability, as compared to commercial carbon/graphite materials, has become the key issue in the development of the electric vehicle industry [1].

Spinel $Li_4Ti_5O_{12}$ is regarded as an alternative anode material for lithium-ion batteries due to its appealing features such as "zero-strain" structure characteristic, stable operating voltage (1.55 V vs. Li/Li^+), good cycling stability, safety, and simple synthesis [2–4]. Therefore, a single cell with an operating voltage of about 2.5 V can be provided when $Li_4Ti_5O_{12}$ couples with high-voltage cathode materials such as $LiCoO_2$, $LiMn_2O_4$, $Li[Li_{0.1}Al_{0.1}Mn_{1.8}]O_4$, and $LiNi_{1/3}Mn_{1/3}Co_{1/3}O_2$, meaning 12 V batteries can be made connecting five cells in series [5–8] so that the batteries can be used as power sources for hybrid electric vehicles (HEV) or plug-in HEV.

Despite many advantages associated with $Li_4Ti_5O_{12}$, low electric conductivity prohibits its use in large-scale applications. Therefore, many strategies have been employed to enhance the electric conductivity of $Li_4Ti_5O_{12}$. Compared with other optimization methods, carbon doping has been proved as an effective and feasible way. Luo et al. [9] synthesized $Li_4Ti_5O_{12}$/C nanorods by a wet-chemical route using glucose as carbon source. Chen et al. [10] prepared $Li_4Ti_5O_{12}$-KB composites by ultrasonication-assisted sol-gel method using $Ti(OC_4H_9)_4$, $LiCH_3COO{\cdot}2H_2O$, and conductive carbon black as the raw materials. Ni et al. [11] prepared nano-$Li_4Ti_5O_{12}$/CNT composites by a liquid-phase deposition method using acetic acid as the chelating agent. In addition,

$Li_4Ti_5O_{12}$/C derived from other carbon sources such as organic acids [12, 13] and polymers [14, 15] were examined. However, previous studies [9–15] mainly focused on the synthesis of $Li_4Ti_5O_{12}$/C composite materials by adding extra carbon sources. The extra carbon sources are added, resulting in relatively complex synthesis process and inconsistency in product quality.

In this work, spinel $Li_4Ti_5O_{12}$/C composites were synthesized by one-step solid-state reaction using lithium lactate ($C_3H_5O_3Li$) as lithium and carbon sources and TiO_2 as a titanium source. The facile one-step synthesis can reduce production steps, contribute to uniform mixing of raw materials, and get homogenous $Li_4Ti_5O_{12}$/C composites. Moreover, as-prepared $Li_4Ti_5O_{12}$/C composites with low in situ carbon content of only 1.81 wt% show significant improvement in discharge capacity and high rate cycling performance comparable to $Li_4Ti_5O_{12}$/C prepared by solid-state reaction in previous studies.

Experimental

The $Li_4Ti_5O_{12}$/C composites were synthesized from a stoichiometric amount of TiO_2 and $C_3H_5O_3Li$ as raw materials. The raw materials were mixed in ethanol as disperser and then ball-milled for 6 h. Subsequently, the mixtures were dried and sintered at 300, 600, and 800 °C for 1, 2, and 8 h in flowing nitrogen, followed by cooling down to room temperature. The final $Li_4Ti_5O_{12}$/C composites were obtained by grinding. As a comparison, pristine $Li_4Ti_5O_{12}$ was prepared using similar method but heated in air.

Electrochemical properties of the $Li_4Ti_5O_{12}$/C composites were evaluated using 2032 coin cells with a lithium metal foil as the counter electrode. The $Li_4Ti_5O_{12}$/C working electrodes were made by mixing active materials, conductive carbon black, and an aqueous binder LA132 (Indigo, China) in a weight ratio of 85:10:5 and then pasted uniformly onto a copper foil and dried at 80 °C under vacuum for 4 h to give the electrodes. The cells were assembled in an argon-filled dry glove box. The electrolyte was a 1.0 mol L^{-1} $LiPF_6$ solution in the mixture of ethylene carbonate, dimethyl carbonate, and ethylene methyl carbonate (1:1:1 by volume). A Celgard 2400 polypropylene membrane was used as the separator.

Thermogravimetric (TG) analysis was performed by a Shimadzu TA-50 thermal analyzer with a heating rate of 10 °C min^{-1} from 30 to 950 °C at a nitrogen flow rate of 50 mL min^{-1}. X-ray diffraction (XRD) was carried on a Shimadzu XRD-7000S X-ray diffractometer with Cu-Kα radiation of λ=1.5418 Å in the range of $10°<2\theta<90°$. Scanning electron microscopy (SEM) was characterized on a FEI Quanta 450 scanning electron microscope. Transmission electron microscopy (TEM) was revealed by a FEI Tecnai G20 transmission electron microscope. The amount of carbon in the $Li_4Ti_5O_{12}$/C composites was measured by a EuroVector EA3000 elemental analyzer. Raman spectra were recorded using a confocal Micro-Raman spectroscopy fitted with a 632.8-nm He-Ne excitation laser. Electrochemical impedance spectra (EIS) were performed by an Autolab PGSTAT 128N in the frequency range from 10^{-1} to 10^6 Hz. Constant current charge-discharge and cycle performance of the cells were tested on a land battery tester and cyclic voltammograms were investigated by an Autolab PGSTAT 128N. All the tests were carried out at room temperature.

Results and discussion

The TG-DTG curves of the precursor mixtures consisting of $C_3H_5O_3Li$ and TiO_2 are shown in Fig. 1. A small peak at 141.69 °C is observed, relating to the removal of adsorbed water. A continuous weight loss between 300 and 600 °C can be related to the thermal decomposition of the precursor. There are two obvious peaks at 301.69 and 456.69 °C, which is relevant to the thermal decomposition of $C_3H_5O_3Li$. When the temperature exceeds 700 °C, the TG curve shows nearly constant weight, indicating that the reaction is complete and well-crystallized $Li_4Ti_5O_{12}$ is obtained. Currently, $Li_4Ti_5O_{12}$/C composites (or $Li_4Ti_5O_{12}$) were synthesized by high-temperature solid-state reaction using TiO_2 as titanium source and different lithium sources. Different lithium sources lead to small differences in decomposition temperatures of solid-state reaction (DTSSR). Inorganic lithium sources include Li_2CO_3 (DTSSR >460 °C) [16, 17], LiOH (DTSSR >500 °C) [18], and $LiNO_3$ (DTSSR >560 °C) [19]. Organic lithium compounds include LiAc (>470 °C) [20] and LiOAc (>320 °C) [21]. Polymer lithium sources include PAALi (>420 °C) [22]. Compared with the above lithium sources, $C_3H_5O_3Li$ shows lower DTSSR, indicating that the synthesis route using $C_3H_5O_3Li$ as lithium source consumes less energy which is beneficial to industrial production and worthy of further investigation.

Figure 2 presents the XRD patterns of the $Li_4Ti_5O_{12}$/C composites and pristine $Li_4Ti_5O_{12}$. It can be seen that all the diffraction peaks between 10 and 90 °C can be indexed to the standard $Li_4Ti_5O_{12}$ pattern (PDF no. 49–0207), demonstrating the obtained samples have a cubic spinel phase structure with no evidence of impurities. This means that the carbon derived from $C_3H_5O_3Li$ does not affect the structure of $Li_4Ti_5O_{12}$ during the heat treatment. The unchanged structure characteristic of $Li_4Ti_5O_{12}$/C ensures its excellent electrochemical cycling performance as pristine $Li_4Ti_5O_{12}$. In addition, there are no obvious diffraction peaks of the carbon in XRD patterns because of its low content or amorphous state.

Figure 3a, b shows the SEM images of the as-prepared $Li_4Ti_5O_{12}$/C and $Li_4Ti_5O_{12}$ particles. As seen, two samples display regular crystalline morphology. The particle size of

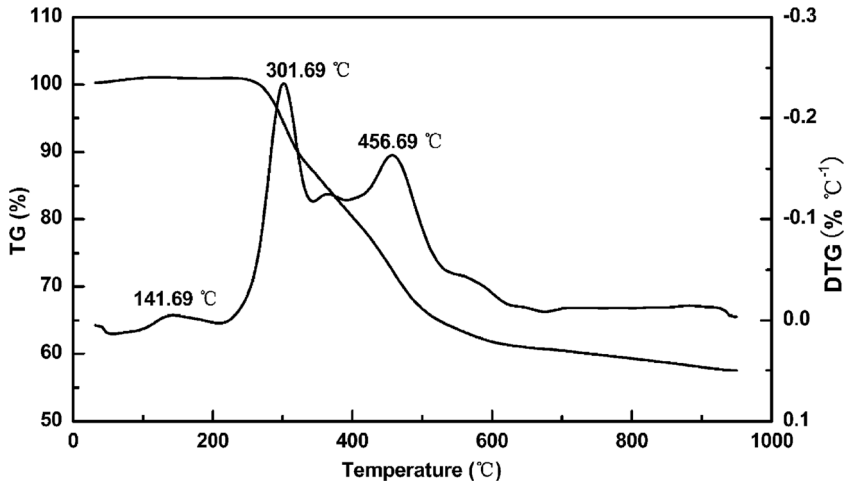

Fig. 1 TG-DTG curves of the $Li_4Ti_5O_{12}$/C precursor

$Li_4Ti_5O_{12}$/C is much smaller than that of $Li_4Ti_5O_{12}$, which exhibits that the in situ carbon from the pyrolysis of $C_3H_5O_3Li$ can effectively prevent the growth of particles during sintering process. And the smaller particles of $Li_4Ti_5O_{12}$/C are more likely to fuse together into larger agglomerates. Usually, it is considered that a smaller $Li_4Ti_5O_{12}$ particle size will shorten lithium-ion diffusion path and contribute to better electrochemical properties. Moreover, the carbon materials can improve electrode performances from some aspects. However, on the other hand, the higher the inactive materials (carbon) content is, the lower the discharge capacity is. It is very important to decrease the inactive materials to balance electrode capacity and other performance for practical use [23, 24]. Currently, the common in situ carbon content in the prepared $Li_4Ti_5O_{12}$/C composites via solid-state reaction is no less than 3 wt% [25–28]. In this work, the content of in situ carbon in the $Li_4Ti_5O_{12}$/C composites is 1.81 wt% measured by elemental analysis. Because the in situ carbon content is lower than those reported in previous studies, it is expected that the discharge capacity and related performances of the $Li_4Ti_5O_{12}$/C composites are better than those in previous studies. In order to observe the detail distribution of the carbon and further verify the particle size and microstructure, the composites were closely studied by TEM. As shown in Fig. 3c, it can be clearly seen from the micrograph that the $Li_4Ti_5O_{12}$ particles are wrapped with an amorphous carbon web, which is consistent with the conclusions of XRD and elemental analysis. Combined with the before-mentioned morphology analysis, the $Li_4Ti_5O_{12}$/C composites are expected to give excellent electrochemical performances.

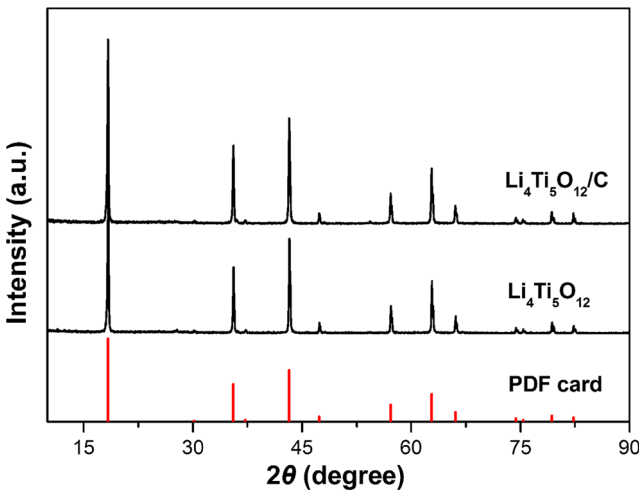

Fig. 2 XRD patterns of the $Li_4Ti_5O_{12}$/C composites and pristine $Li_4Ti_5O_{12}$

Figure 4 shows the Raman spectra of the $Li_4Ti_5O_{12}$/C composites. The intense broadbands at about 1325 and 1591 cm^{-1} are assigned to the disorder (D) and graphene (G) bands of in situ carbon in $Li_4Ti_5O_{12}$/C composites, respectively. The G band corresponds to one of the E_{2g} modes, which has been assigned as the sp^2 graphite-like structure, whereas the D band corresponds to one of the A_{1g} modes, which is attributed to the sp^3 type tetrahedral carbon. The value I_D/I_G (the peak intensity ratio) can be used to evaluate the content of sp^{3-} and sp^{2-} coordinated carbon in the sample, as well as the degree of disorder for the in situ carbon. Theoretically, the high values for the I_D/I_G and A_{sp3}/A_{sp2} (the area ratio of sp^{3-} to sp^{2-} coordinated carbon) parameters indicate a low degree of graphitization [9]. The value of the I_D/I_G ratio of 1.17 is calculated. It suggests that the in situ carbon is mainly in an amorphous structure, which is consistent with the conclusions of TEM.

Figure 5 shows the cyclic voltammograms (CVs) of the as-prepared $Li_4Ti_5O_{12}$/C and $Li_4Ti_5O_{12}$ electrodes. It is obvious that both samples show a pair of sharp redox peaks, which are the characteristics redox peaks of $Li_4Ti_5O_{12}$. At a scan rate of 0.2 mV s^{-1}, it should be noted that the redox peak profile is located at 1.46/1.68 V for the $Li_4Ti_5O_{12}$/C, and 1.36/1.73 V for the $Li_4Ti_5O_{12}$. The $Li_4Ti_5O_{12}$/C electrode has a smaller potential separation compared with the $Li_4Ti_5O_{12}$ electrode, showing a smaller polarization. This could be attributed to the

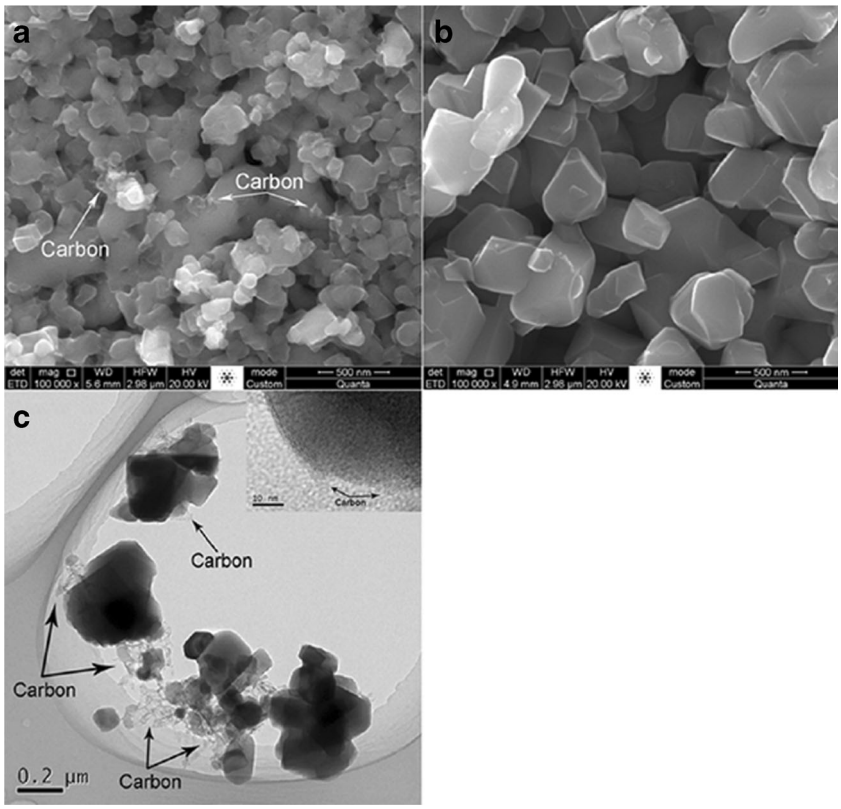

Fig. 3 SEM image of the $Li_4Ti_5O_{12}$/C (**a**) and $Li_4Ti_5O_{12}$ (**b**) and TEM image (**c**) of the $Li_4Ti_5O_{12}$/C

following reasons. First, the smaller size makes shorter distance for lithium-ion diffusion in $Li_4Ti_5O_{12}$/C particles and benefits the diffusion process. Moreover, the in situ carbon in $Li_4Ti_5O_{12}$/C composites effectively improves the electrical contact of each $Li_4Ti_5O_{12}$ particle, thus enhancing electrochemical performances of $Li_4Ti_5O_{12}$. These results are consistent with the conclusions of SEM and TEM micrographs.

Figure 6 presents EIS of $Li_4Ti_5O_{12}$/C and $Li_4Ti_5O_{12}$ cells. It can be seen that the $Li_4Ti_5O_{12}$/C cell exhibits much lower impedance than the $Li_4Ti_5O_{12}$ cell, indicating much better electronic conductivity of the $Li_4Ti_5O_{12}$/C composites. According to the formula $\sigma = d/AR$ (where σ is the conductivity, R is the resistance, d is the thickness, and A is the specific surface area) [29], the electronic conductivities of $Li_4Ti_5O_{12}$

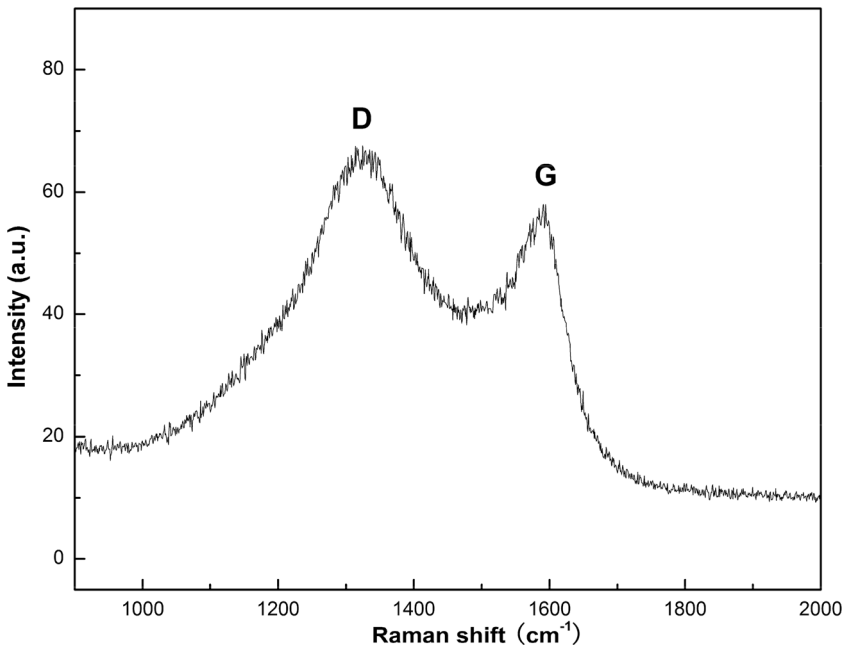

Fig. 4 Raman spectra of the $Li_4Ti_5O_{12}$/C composites

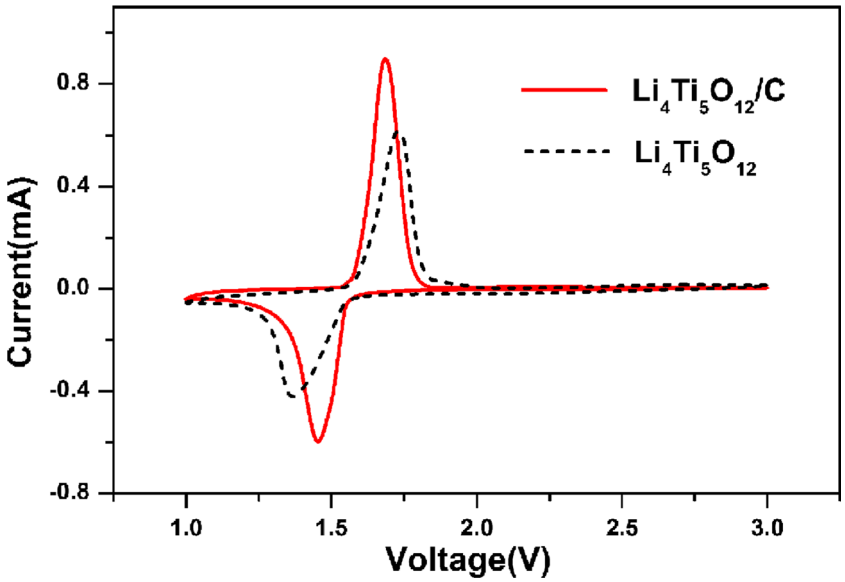

Fig. 5 CVs of the $Li_4Ti_5O_{12}$/C and $Li_4Ti_5O_{12}$ electrodes

and $Li_4Ti_5O_{12}$/C are 8.4×10^{-8} and 1.8×10^{-7} S cm^{-1}, respectively. The increase of the electronic conductivity in the $Li_4Ti_5O_{12}$/C composite is mainly due to the presence of pyrolytic carbon. As a result, the redox polarization decreases from 40 to 37 mV based on the charge-discharge curves at 0.2 C. Cycled at 20 C, the insertion/extraction polarization reduces from 532 to 373 mV as shown in Fig. 7. These facts are consistent with the results of CVs. Furthermore, with the increase of current density, the electrode polarization increases gradually and the discharge capacity gradually decreases as shown in Fig. 7. At a low rate of 0.2 C, the initial discharge capacity of 168.4 mAh g^{-1} is delivered for the sample (it is 171.5 mAh g^{-1} if the capacity is calculated based on the weight of the $Li_4Ti_5O_{12}$ in the $Li_4Ti_5O_{12}$/C electrode), which is close to its theoretical capacity of 175.0 mAh g^{-1}. At high current rates of 10 C and 20 C, the samples still show 140.0 and 133.3 mAh g^{-1}, respectively. Some results of previous works on the $Li_4Ti_5O_{12}$/C prepared by solid-state reaction are listed in Table 1. When total carbon content is similar, the discharge capacity of $Li_4Ti_5O_{12}$/C using $C_3H_5O_3Li$, especially at high rates, is better than the results listed in Table 1. It was worth noting that carbon-free $Li_4Ti_5O_{12}$ electrode showed excellent electrochemical performance both in the rate capability and the long-term cyclability, and the electrode delivers 9 % higher capacity than carbon composite electrode in ref. [31]. The idea of ref. [31] is essentially consistent with our concept that very low carbon content in the $Li_4Ti_5O_{12}$ electrode. Does $Li_4Ti_5O_{12}$ need carbon in lithium-ion batteries?

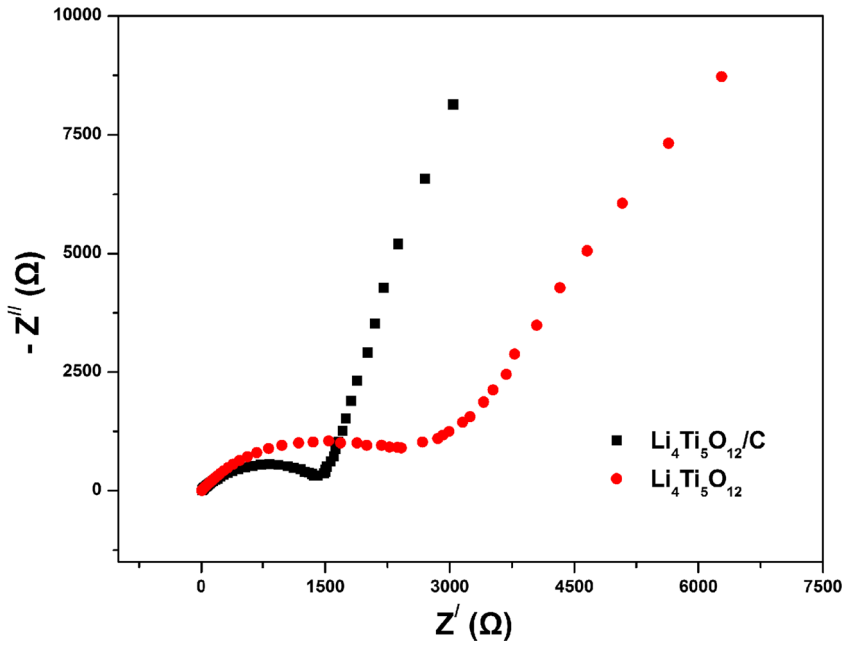

Fig. 6 EIS of the $Li_4Ti_5O_{12}$/C and $Li_4Ti_5O_{12}$ cells

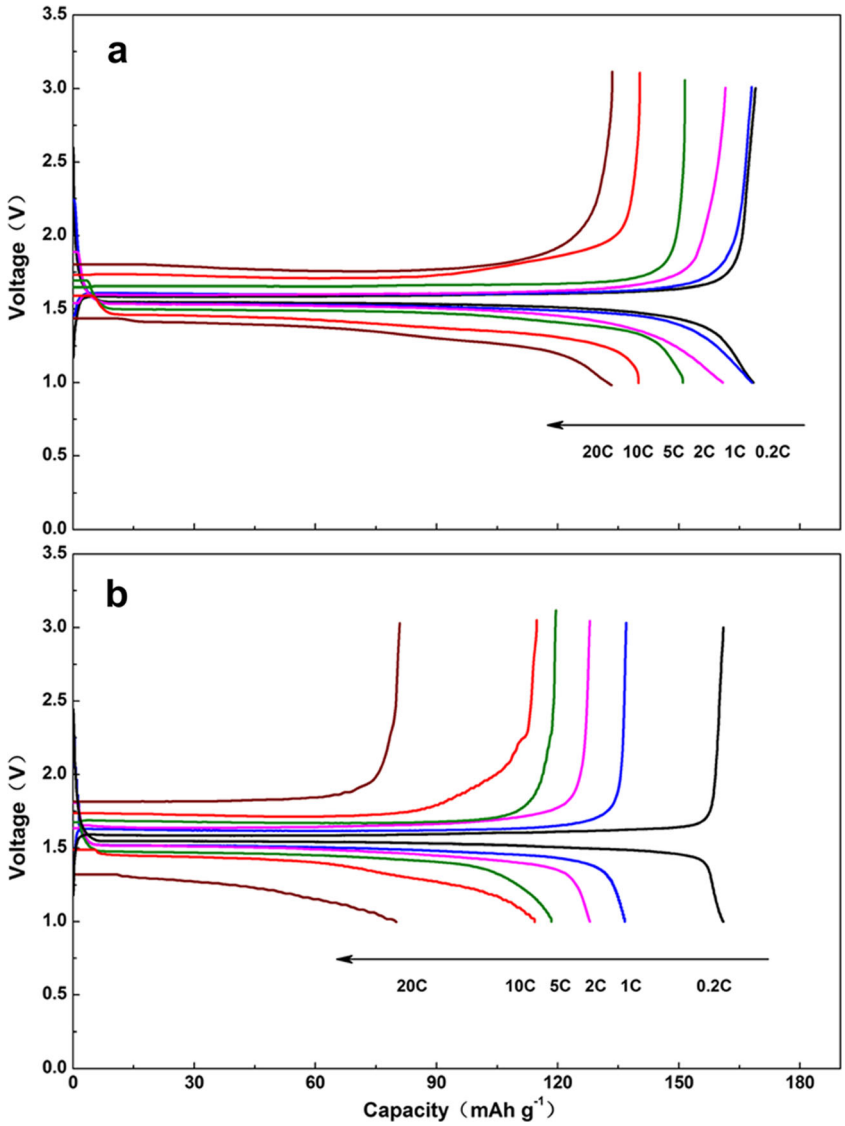

Fig. 7 The first charge-discharge curves of the $Li_4Ti_5O_{12}$/C composites (**a**) and pristine $Li_4Ti_5O_{12}$ (**b**) at different rates

The answer is yes. Firstly, the high rate capability of $Li_4Ti_5O_{12}$ is one of its most important advantages as an anode material. As shown in Fig. 3a (ref. [31]), the discharge capacities of the carbon-containing $Li_4Ti_5O_{12}$ electrode gradually exceeded those of the carbon-free $Li_4Ti_5O_{12}$ electrode when charge-discharge rate reached 3 C. With the increase of the charge-discharge rate, reversible capacity decay of the carbon-containing $Li_4Ti_5O_{12}$ electrode was significantly less than that of the carbon-free $Li_4Ti_5O_{12}$ electrode, which illustrated that the carbon helped to improve high rate discharge capacity. Secondly, high coulombic efficiency is important for the electrode materials. As shown in Fig. 3a (ref. [31]), with the increase of the charge-discharge rate, coulombic efficiencies of the carbon-containing $Li_4Ti_5O_{12}$ electrode were significantly higher than those of the carbon-free $Li_4Ti_5O_{12}$ electrode, which indicated that the carbon helped to improve high rate cycling performance. Compared with ref. [31], further research has been done in our work. At high rates (>2 C), the discharge capacities of $Li_4Ti_5O_{12}$/C electrode are significantly higher than those of ref. [31], which is due to the presence of carbon in the as-prepared $Li_4Ti_5O_{12}$/C. Moreover, $Li_4Ti_5O_{12}$/C electrode at high rates provides high coulombic efficiencies close to 100 %, which is significantly higher than those of ref. [31] (see Fig. S4 in the reference. 2 C: 94.0 %[a], 5 C: 83.0 %[a], 10 C: 72.0 %[a]). These results show that the $Li_4Ti_5O_{12}$/C composites have high rate capacity, which is due to the low in situ carbon content in them, indicating that lithium lactate is indeed suitable lithium and carbon sources for the one-step solid-state synthesis of $Li_4Ti_5O_{12}$/C composites. Moreover, it can be expected that the $Li_4Ti_5O_{12}$/C composites provide better high rate capability because of its higher electronic conductivity compared with the pristine $Li_4Ti_5O_{12}$.

The rate performances of the $Li_4Ti_5O_{12}$/C composites and pristine $Li_4Ti_5O_{12}$ at different rates are shown in Fig. 8. It can be seen that the $Li_4Ti_5O_{12}$/C composites have high rate performance though the reversible capacities decreased gradually

Table 1 Discharge capacities, carbon contents, and capacity retention of $Li_4Ti_5O_{12}$/C prepared by solid-state reaction in the reference works

Reference	Discharge capacity (mAh g^{-1})				Carbon content (wt%)			Capacity retention
	0.2 C	1 C	10 C	20 C	C content in $Li_4Ti_5O_{12}$/C	Conductive C content	Total carbon content	
Our work	168.4	168.0	140.0	133.3	1.87	10.0	11.59	1 C: 94.4 % (200th) 10 C: 90.2 % (200th)
Ref. [32]	140.0[a]	130.0[a]	80.0[a]	–	0.4	10.0	10.32	–
	171.0[a]	162.0[a]	124.0[a]		1.8		11.44	
	150.0[a]	138.0[a]	90.0[a]		9.6		17.68	
Ref. [33]	–	162.2	118.9	78.7	1.82	10.0	11.55	–
		167.7	134.9	115.7	2.75		12.34	
		103.6	27.0[a]	–	5.38		14.57	
Ref. [25]	162.0[a]	153.6	115.0	–	5.16	10.0	14.13	1 C: 97.7 % (200th)[a]
Ref. [26]	165.6 (0.1 C)	151.4	117.5 (5 C)	–	3.0	10.0	12.4	1 C: 97.1 % (200th)[a]
	162.4 (0.1 C)	147.4	114.9 (5 C)		5.0		14.0	1 C: 94.3 % (200th)[a]
Ref. [27]	–	129.9	–	–	2.8	10.0	12.24	1 C: 90.8 % (50th)[a]
		153.1			4.6		13.68	1 C: 97.3 % (50th)[a]
		142.4			6.7		15.36	1 C: 93.4 % (50th)[a]
Ref. [34]	–	154.0	121.0	110.0	2.90	8.0	10.47	–
Ref. [35]	176.2	162.0	136.7	121.1	low	10.0	>10.0	1 C: 92.5 % (100th) 10 C: 91.8 % (100th)
Ref. [28]	–	188.0[a]	112.0[a]	69.0[a]	5.0	5.0	10.0	–
		168.0[a]	87.0[a]	51.0[a]	7.5	2.5		
		179.0[a]	71.0[a]	36.0[a]	10.0	0		
Ref. [30]	–	149.0[a]	130.0[a]	118.0[a]	2.48	7.5	9.98	1 C: 98.0 % (200th)[a]
Ref. [31]	160.0[a]	154.5[a]	115.0[a]	–	0	5	5	1 C: 98.0 % (100th)[a]
	162.5[a]	157.5[a]	112.5[a]	–	0	0	0	1 C: 96.5 % (100th)[a]

Discharge capacity is calculated based on the weight of the active materials ($Li_4Ti_5O_{12}$/C) in the electrodes

[a] The values from the pictures in the references

with the increase of current density. Moreover, the $Li_4Ti_5O_{12}$/C composites demonstrate obviously improved reversible capacity and rate performance over the pristine $Li_4Ti_5O_{12}$, especially at higher current rates. Even at 20 C, the discharge capacity still reaches 109.8 mAh g^{-1} after 50 cycles, while for pristine $Li_4Ti_5O_{12}$, the corresponding value is 43.5 mAh g^{-1}. The results show that the $Li_4Ti_5O_{12}$/C composites exhibit excellent rate performance, which is attributed to

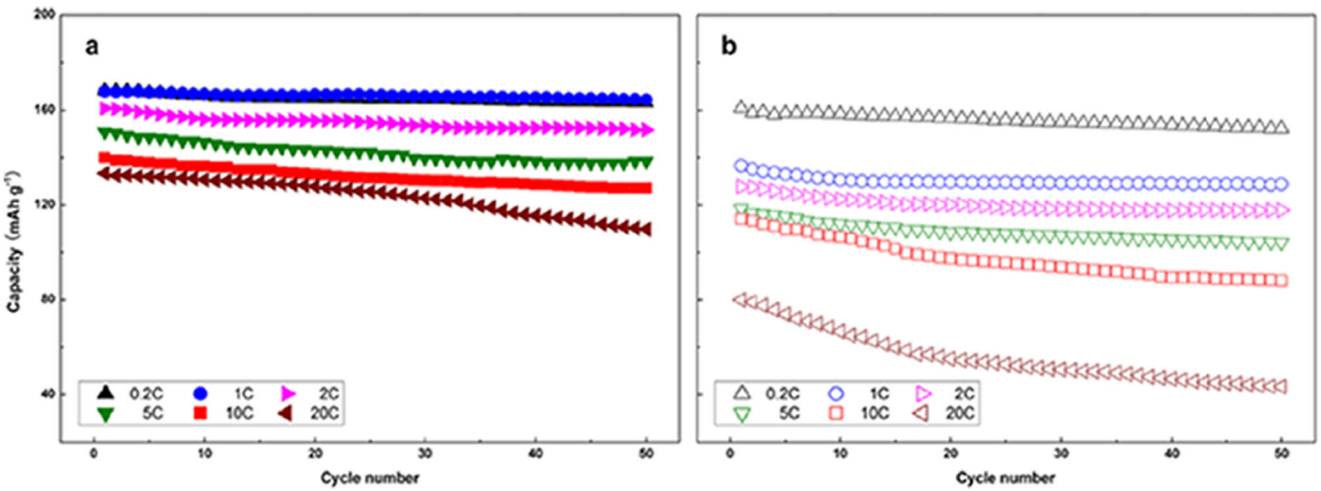

Fig. 8 The rate performance of the $Li_4Ti_5O_{12}$/C composites (**a**) and pristine $Li_4Ti_5O_{12}$ (**b**) at different rates

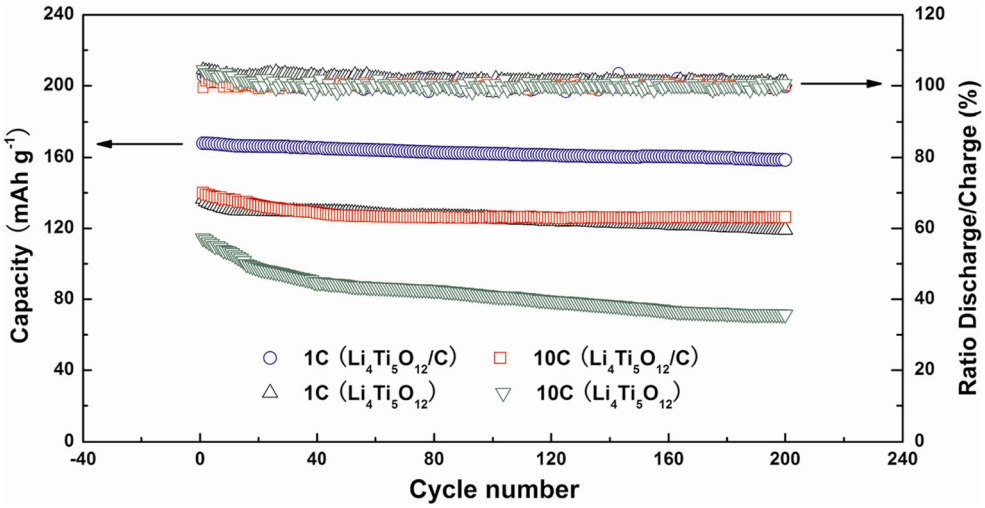

Fig. 9 The cycle curves of the $Li_4Ti_5O_{12}$/C composites and pristine $Li_4Ti_5O_{12}$ at 1 C and 10 C

the amorphous carbon layer on the surface of $Li_4Ti_5O_{12}$. The pyrolytic carbon webs derived from $C_3H_5O_3Li$ increase the electronic conductivity of $Li_4Ti_5O_{12}$, and hence improve its electrochemical properties, especially the high rate capability.

Figure 9 shows the cycling performance of the $Li_4Ti_5O_{12}$/C composites and pristine $Li_4Ti_5O_{12}$ at 1 C and 10 C. The $Li_4Ti_5O_{12}$/C composites and pristine $Li_4Ti_5O_{12}$ both provide high coulombic efficiencies close to 100 %. At a low rate of 1 C, the initial capacity is 168.0 mAh g^{-1} with capacity retention of 94.4 % at 200th cycle for the $Li_4Ti_5O_{12}$/C composites, while for pristine $Li_4Ti_5O_{12}$, the corresponding values are 136.6 mAh g^{-1} and 87.2 %, respectively. At a high rate of 10 C, the initial capacity is 140.0 mAh g^{-1} with capacity retention of 90.2 % at 200th cycle for the $Li_4Ti_5O_{12}$/C composites, while for pristine $Li_4Ti_5O_{12}$, the corresponding values are 114.3 mAh g^{-1} and 62.5 %, respectively. Compared with previous studies listed in Table 1, the $Li_4Ti_5O_{12}$/C composites in this work exhibit excellent low rate cycling performance the same as those in previous studies. Furthermore, their high rate cycling performance is better than those of $Li_4Ti_5O_{12}$/C in previous studies. The results show that the as-prepared $Li_4Ti_5O_{12}$/C composites exhibit excellent high rate cycling performance, which is attributed to the presence of pyrolytic carbon. The abovementioned electrochemical facts illustrate that low in situ carbon content of the as-prepared $Li_4Ti_5O_{12}$/C composites perfectly balances discharge capacity and high rate cycling performance.

Conclusions

Spinel $Li_4Ti_5O_{12}$/C composites were obtained from $C_3H_5O_3Li$ and TiO_2 via one-step solid-state reaction without adding extra carbon sources. Herein, the commonly used organic lithium salt $C_3H_5O_3Li$ supplies both lithium and carbon sources. The low in situ carbon content of the as-prepared $Li_4Ti_5O_{12}$/C composites perfectly balances discharge capacity and high rate cycling performance. At 0.2 C, the initial discharge capacity of 168.4 mAh g^{-1} is delivered for the sample, which is close to its theoretical capacity of 175.0 mAh g^{-1}. At 1 C and 10 C, the initial capacity is 168.0 and 140.0 mAh g^{-1} with capacity loss of 5.6 and 9.8 % at 200th cycle, respectively. Even at 20 C, the discharge capacity still reaches 109.8 mAh g^{-1} after 50 cycles. As a result, the $Li_4Ti_5O_{12}$/C composites derived from this synthetic route show high discharge capacity and excellent rate cycling performance, which makes them a promising anode candidate for electric vehicles.

Acknowledgments This work was supported by Program for Chongqing Science & Technology Innovation Talents (cstc2013kjrc-qnrc50006), the National Natural Science Foundation of China (No. 21206203, 21306235), and the Scientific Research Innovation Team of Chongqing University of Technology (No. cqut2015srim).

References

1. Chen ZH, Ren Y, Jansen AN, Lin CK, Weng W, Amine K (2013) Nat Commun 4:1513–1520
2. Qiu CX, Yuan ZZ, Liu L, Ye N, Liu JC (2013) J Solid State Electrochem 17:841–847
3. Zhao YY, Pang SP, Li HS, Zhang CJ, Zhang QH, Gu L, Zhou XH, Li GC, Cui GL (2013) J Solid State Electrochem 17:1479–1485
4. Zhang HQ, Deng QJ, Mou CX, Huang ZL, Wang Y, Zhou AJ, Li JZ (2013) J Power Sources 239:538–545
5. Yi TF, Yang SY, Xie Y (2015) J Mater Chem A 3:5750–5777
6. Nakura K, Ariyoshi K, Yoshizawa H, Ohzuku T (2015) J Electrochem Soc 162:A622–A628
7. Wang LN, Nakura K, Imazaki M, Kakizaki N, Ariyoshi K, Ohzuku T (2012) J Electrochem Soc 159:A1710–A1715
8. Nagayama M, Ariyoshi K, Yamamoto Y, Ohzuku T (2014) J Electrochem Soc 161:A1388–A1393
9. Luo HJ, Shen LF, Rui K, Li HS, Zhang XG (2013) J Alloys Compd 572:37–42
10. Chen SL, Wu HB, Hu HC, Mo YH, Yin JL, Wang GL, Cao DX, Zhang YM, Yang BF, She PL (2013) Solid State Ionics 233:1–6
11. Ni HF, Fan LZ (2012) J Power Sources 214:195–199

12. Yang GL, Su Z, Fang HS, Yao YC, Li YM, Yang B, Ma WH (2013) Electrochim Acta 93:158–162
13. Gu F, Chen G (2012) Int J Electrochem Sci 7:6168–6179
14. Yang ZX, Meng Q, Guo ZP, Yu XB, Guo TL, Zeng R (2013) Energy 55:925–932
15. Fang W, Cheng XQ, Zuo PJ, Ma YL, Liao LX, Yin GP (2013) Solid State Ionics 244:52–56
16. Wang L, Zhang ZL, Liang GC, Ou XQ, Xu YQ (2012) Powder Technol 215–216:79–84
17. Yang LX, Gao LJ (2009) J Alloys Compd 485:93–97
18. Gao L, Qiu WH, Zhao HL (2005) J Univ Sci Technol Bejing 1:82–85
19. Abe Y, Matsui E, Senna M (2007) J Phys Chem Solids 68:681–686
20. Wu HL, Huang YD, Jia DZ, Guo ZP, Miao M (2012) J Nanoparticle Res 14:713
21. Wang L, Xiao QZ, Li ZH, Lei GT, Zhang P, Wu LJ (2012) J Solid State Electrochem 16:3307–3313
22. Lin ZJ, Hu XB, Huai YJ, Liu L, Deng ZH, Suo JS (2010) Solid State Ionics 181:412–415
23. Marks T, Trussler S, Smith AJ, Xiong DJ, Dahn JR (2011) J Electrochem Soc 158:A51–A57
24. Fongy C, Moreau P, Chazelle S, Bouvier M, Jounanneau S, Guyomard D, Lestriez B (2012) J Electrochem Soc 159:A1083–A1090
25. Li HS, Shen LF, Zhang XG, Wang J, Nie P, Che Q, Ding B (2013) J Power Sources 221:122–127
26. Li BH, Ning F, He YB, Du HD, Yang QH, Ma J, Kang FY, Hsu CT (2011) Int J Electrochem Sci 6:3210–3223
27. Gao J, Jiang CY, Wang CR (2010) Ionics 19:417–424
28. Zheng XD, Dong CC, Huang B, Liu M (2013) Ionics 19:385–389
29. Shu J, Hou L, Ma R, Shui M, Shao LY, Wang DJ, Ren YL, Zheng WD (2012) RSC Adv 2:10306–10309
30. Cheng L, Yan J, Zhu GN, Luo JY, Wang CX, Xia YY (2010) J Mater Chem 20:595–602
31. Song MS, Benayad A, Choi YM, Park KS (2012) Chem Commun 48:516–518
32. Zhu ZQ, Cheng FY, Chen J (2013) J Mater Chem A 1:9484–9490
33. Tang JX, Gao LJ (2012) Phys Scr 85:045802
34. Yuan T, Cai R, Shao ZP (2011) J Phys Chem C 115:4943–4952
35. Zheng SW, Xu YL, Zhao CJ, Liu HK, Qian XZ, Wang JH (2012) Mater Lett 68:32–35